

Scanning tunneling spectroscopy on oxidized surfaces of highly resistive quasicrystalline alloysJ. Delahaye,^{1,*} T. Schaub,¹ C. Berger,^{1,†} and Y. Calvayrac²¹LEPES-CNRS, Avenue des Martyrs, Boite Postal 166, 38042 Grenoble Cedex 9, France²CECM-CNRS, 15 rue Georges Urbain, 94407 Vitry sur Seine Cedex, France

(Received 4 December 2002; published 6 June 2003)

We report on a detailed investigation of the one-electron density of states on oxidized surfaces of highly resistive quasicrystalline alloys. Scanning tunneling spectroscopy measurements were performed at low temperatures (resolution around 5 meV) on icosahedral (*i*-)AlPdMn, *i*-AlCuFe, and *i*-AlPdRe. The tunneling spectra depend largely on the scanning tunneling microscope tip location on the oxidized surfaces. Beside spectra characteristic for the Coulomb blockade, we have identified a zero bias dip intrinsic to our quasicrystalline samples. This single feature increases as a square root of the bias voltage up to ≈ 100 mV. A natural explanation comes from the combined effects of electron-electron interactions and disorder on the one-electron density of states. In this respect, highly resistive icosahedral alloys behave similar to disordered systems, for which such singularity has been predicted and widely observed. We have found no evidence for the quasicrystal specific energy dependence which was expected from anomalous diffusion laws predicted by quasiperiodic models. The predicted multiple gap structure has not been found either. We discuss which density of states is actually measured in tunneling spectroscopy to help clarify the controversial results obtained in this field.

DOI: 10.1103/PhysRevB.67.214201

PACS number(s): 71.30.+h, 71.23.Ft, 72.15.-v

I. INTRODUCTION

One of the most spectacular properties of quasicrystals (QC's) is the high electrical resistivity ρ experimentally observed in a number of Al-based icosahedral (*i*) alloys containing transition metals.¹ For example, the resistivity at 4 K can reach 10 m Ω cm in *i*-AlCuFe and *i*-AlPdMn samples, and even more than 1 Ω cm in some *i*-AlPdRe samples, which were found to be already on the insulating side of a metal-insulator (MI) transition.² One related property is the electronic density of states (DOS), which has been so far an active field of research, both experimentally and theoretically.

In highly resistive icosahedral and approximant phases, a consensual feature of the DOS is the presence of a broad pseudogap, about 1 eV wide around the Fermi level (E_F). It has been observed both in theoretical calculations and experiments, such as soft x-ray spectroscopy,³ x-ray photoemission spectroscopy (XPS),⁴⁻⁷ optical properties,⁸⁻¹⁰ and specific-heat measurements.^{11,12} For instance, the electronic contribution to the specific heat is lower than that of pure Al by a factor of 1/3 in *i*-AlPdMn (Ref. 13) and *i*-AlCuFe (Ref. 14) samples, and more than 1/10 in the most resistive *i*-AlPdRe samples.^{15,16} This electronic depletion is attributed to the Hume-Rothery mechanism.

However, this reduction in electrons at and around the Fermi level could not account alone for the high-resistivity values observed in some icosahedral alloys and approximants. A possible explanation is given by linear muffin-tin orbital (LMTO) calculations on icosahedral approximants with a realistic atomic model at the real alloy composition.¹⁷ The calculated DOS displays around the Fermi level an unusual set of peaks and pseudogaps of typical energy widths between 1 meV and 100 meV. This fine structure is associated with bands of small-energy dispersion, yielding a low group velocity for the electron wave packets that could ex-

plain the high-resistivity values. Further theoretical work has suggested that this so-called fine structure could stem from the presence of clusters of transition metals in the structure.¹⁸ Extending the idea of atomic virtual bound states to a cluster, Trambly *et al.* have investigated a cluster of transition-metal atoms in an Al jellium. They have found a sharper resonance structure than for isolated transition-metal atoms. The lifetime associated with these states is increased and so is the resistivity. Another property that follows from the fine structure (and the related electron confinement) is the strong sensitivity of the resistivity values to the chemical composition or local order. As the electrons are partially localized in cluster virtual bound states, a small change of the clusters chemical composition or local order from the ideal one will lead to a more conducting system. Such sensitivity was actually observed experimentally.^{11,19,20} Let us, however, mention that the existence of this fine structure in icosahedral models with an infinite unit cell has been recently questioned on theoretical grounds.²¹

Several experiments have tried to unveil this DOS feature, which could reveal QC specific properties. Changes in the thermoelectric power with temperature and *i*-phase composition²² and nuclear magnetic relaxation times with temperature²³ have been interpreted by sharp variations of conductivity and DOS with energy. However, this is an indirect evidence, since variations with energy are scanned by temperature sweeps, and other phenomena could occur. Spectroscopic measurements of the DOS close to E_F at the required resolution (i.e., at least 100 meV) yielded confused results in the literature. XPS data^{4,5} indicate a single fine pseudogap located at the Fermi level, but the energy dependence and the amplitude of the DOS reduction vary mainly due to a different surface quality of the measured samples. Tunneling spectroscopy experiments²⁴⁻²⁶ also confirmed a single dip at the Fermi level, but there again the spectral dependence varies for different experiments. In a tunneling

spectroscopy study of a decagonal single grain, a set of peaks and pseudogaps was also observed,²⁷ but it was later shown that this was most probably due to superconducting effects of the counterelectrode.²⁸ In fact, the discrimination between QC intrinsic effects and extrinsic effects appears to be an issue in tunneling spectroscopy studies of QC's.

Another fundamental question in QC's is the existence or not of an anomalous spreading of wave packets with time, as found in exact numerical studies of quasiperiodic systems.^{29–33} Indeed, it is found that the propagation is, in general, neither ballistic such as in perfect crystals, nor diffusive such as in disordered systems. The spreading length rather grows at time long enough as $L(t) \propto t^\beta$. The exponent β varies between 0 and 1, depending on the Hamiltonian parameters and the energy considered. This anomalous spreading is a direct signature of quasiperiodicity, but has so far received no indubitable experimental support. Evidence has been searched for in the temperature dependence of the electrical conductivity, where anomalous exponents β could give specific power laws. Power laws have indeed been observed in highly resistive icosahedral alloys,¹² such as *i*-AlPdMn, *i*-AlCuFe, or *i*-AlPdRe, but the determined exponents are similar to those of disordered systems with similar resistivity values. Another indication of this anomalous spreading law may be searched for in the one-electron DOS close to the Fermi level. This last point has to our knowledge never been addressed experimentally before, and will be discussed in more details in this paper.

In this paper, we present a different scanning tunneling spectroscopy (STS) investigation of highly resistive icosahedral samples. We have found evidence for an intrinsic $\sqrt{|E - E_F|}$ singularity in the DOS centered at the Fermi level, which we attribute to electron-electron interactions and localization effects close to the metal-insulator transition. Large spatial fluctuations are measured, which might come to some extent from fluctuations of the chemical composition at the surface. No signature of an anomalous electronic propagation has been found in the voltage dependence of the tunneling spectra. We aim at bringing these measurements into perspective together with previous tunneling spectroscopy results of the literature and in light of theoretical arguments from the point of view of both the QC and the disordered systems. Possible *i*-AlPdRe specificity related to the insulating state is also discussed.

In Sec. II, we introduce relevant tunneling spectroscopy concepts and give details about the samples and experimental setup. Section III provides an overview of our tunneling spectra, which we classify as extrinsic (Sec. IV) or intrinsic effects (Sec. V). In Sec. VI, we discuss previous tunneling spectroscopy experiments in the light of the present study.

II. SCANNING TUNNELING SPECTROSCOPY: PHYSICAL PRINCIPLES AND EXPERIMENTAL SETUP

A. General considerations

1. Planar junction geometry

Tunneling spectroscopy has been applied successfully to a large number of systems to determine the DOS close to the

Fermi level. The most classical geometry is the planar junction, where two planar electrodes are separated by a thin insulating layer, usually an oxide. In the $T=0$ limit, if the coupling between the two electrodes is weak (i.e. high tunneling resistance at small bias voltage U), the tunneling conductance $G(U) = dI/dU$ between a metallic electrode (having a DOS independent of energy) and a sample electrode [having a DOS $N(E)$] follows the relation:³⁴

$$G(U, T=0) \propto N(E_F + eU, T=0). \quad (1)$$

The tunneling conductance at voltage U is thus directly proportional to the sample DOS at energy $E_F + eU$. Usually in metals, $G(U)$ is constant in the range ± 200 mV. When voltage increases and energy eU is no more negligible compared with the barrier height, corrections to relation (1) must be taken into account. The reduction in the effective height of the barrier leads to a parabolic increase of the tunneling conductance with voltage, which becomes stronger at higher voltage.

At finite temperature, we have to take into account the finite probability for states above the Fermi level to be occupied. Relation (1) is then given by

$$G(U, T) \propto \int_0^\infty N(E, T) \frac{\partial f_T(E - eU)}{\partial eU} dE, \quad (2)$$

where f_T is the Fermi-Dirac equilibrium distribution at temperature T . The density of states is noted $N(E, T)$ since, in general, it can have an intrinsic temperature dependence. At a temperature T , the tunneling conductance is thus proportional to the electronic DOS convoluted by the thermal broadening function $-\partial f_T / \partial E$. This leads to an apparent limited resolution of the order of $4k_B T$. If the density of states is smooth on this energy scale or if the only sharp structure is located at the Fermi level, the tunneling conductance (even at nonzero temperature) can be considered as directly proportional to the DOS $N(E_F + eU)$, but only for voltages $|eU| > \approx 4k_B T$. At a known temperature, if the tunneling conductance is measured with sufficient precision, a deconvolution of the data by the thermal broadening function is, in principle, possible. At 4 K, $4k_B T \approx 1$ meV, which is of the order of the narrowest peaks and pseudogaps seen in the electronic DOS calculations on approximant phases. Thus, at this temperature, a fine structure should be observable in the tunneling conductance spectra $G(U)$.

Note that whether the tunneling spectra reflect a property of the bulk electrode or a property of the interface itself will primarily depend on the nature of the states involved (localized versus delocalized states). Indeed, the probed thickness varies, in general, with the bias voltage and also with the system considered. This point will be discussed in more details in Sec. V C for the specific case of highly resistive icosahedral alloys.

2. Choice of a scanning tunneling microscope geometry

In our experiment, we have chosen a different geometry. Instead of a planar junction, we used the metallic tip of a scanning tunneling microscope (STM), which is approached

close enough to the QC surface of interest. Different elements have motivated this choice.

First, in a planar geometry, the tunneling conductance reflects the DOS of the sample but averaged on the area of the junction. In practical realization, the tunneling barrier is not homogeneous and the tunneling current is limited to some constrictions. But the conductance measured there is nevertheless an average over a large surface compared with the lateral resolution provided by a STM tip (typically few angstroms). Averaging might be an issue when dealing with the expected QC fine DOS structure, since the energy location of the peaks and pseudogaps in the DOS calculations are very sensitive to the chemical composition. This implies that if the probed area is not chemically homogeneous, the predicted fine structure could be smoothed out in a planar junction geometry, whereas the STM configuration is more favorable.

Second, the fabrication of high quality planar tunnel junctions on bulk materials such as ribbons, single grains, or even thin films, is not easy. As discussed in Sec. VI, it has yet never been realized on QC's. By high quality, we mean tunneling barriers that are homogeneous and without leaking currents. Al-based QC surfaces are very reactive to oxygen. In ambient conditions, they are covered by an oxide layer that is a few nanometers thick. The electronic properties of this oxide layer are not known, but its composition is closed to Al_2O_3 which is an insulator often used as a tunneling barrier in artificial structures. Since this native grown layer is expected to contain some pinholes, defects, and/or impurities, it cannot be used directly as a tunneling barrier in a planar junction configuration. Our initial idea was therefore to avoid an unreliable additional sample preparation by using a STM tip as the counterelectrode. In this case, the tunneling barrier is obtained directly by the native oxide layer on top of the QC surface and occasionally the vacuum between the tip and the oxide. With a local probe, metallic pinholes or oxide nonhomogeneity should be more scarcely observed. Moreover, the distance between the tip and the sample, and therefore the barrier height, could be changed easily during the experiment. But as discussed below, our study indicates that more reproducible results are obtained when the QC surface is cleaned under UHV and subsequently reoxidized in a controlled oxygen atmosphere.

In a scanning tunneling spectroscopy geometry, relations (1) and (2) have to be modified. The usual approach is the Tersoff-Hamann approximation,³⁵ where the metallic tip is assumed to be a sphere, and the surface of the sample a plane. At $T=0$ and if the coupling between the tip and the surface is low (high tunneling resistance), the tunneling conductance is given by^{36,37}

$$G(U, T=0) \propto N_s(\vec{r}_0, E_F + eU, T=0). \quad (3)$$

The DOS N_s in relation (3) is now the local electronic DOS, defined as

$$N_s(\vec{r}_0, E_F + eU) = \sum_i |\Psi_i(\vec{r}_0)|^2 \delta(E_i - E_F - eU). \quad (4)$$

The main contribution to the tunneling current comes from electronic states i which have a large amplitude of probability Ψ_i at the center \vec{r}_0 of the spherical tip. As already mentioned, it is clear from Eq. (4) that the typical depth probed by the experiment will depend on the nature of the electronic states at the energy considered.

B. Experimental setup

1. Scanning tunneling spectroscopy setup

The scanning tunneling microscope is the same as previously used in the spectroscopy measurements performed by Davydov and co-workers^{24,25} on QC's. Experimental details have already been given elsewhere. We used Pt-Ir tips, prepared by wire stretching. Since the shape of the STM tip is ill controlled, the replacement of the tip moves the scanning area (typically $1 \times 1 \mu\text{m}$) by a few $10 \mu\text{m}$.

The electronic setup is an improved version of the one used by Davydov *et al.*, and in particular, the electrical noise is significantly reduced, although it remains of the order of 5 meV, i.e., above the thermal broadening energy. The tunneling current is measured with a homemade current-voltage converter at room temperature (low noise operational amplifier OPA606). The feedback resistance of the preamplifier can be switched between 20 M Ω and 10 k Ω , so that tunneling resistance junctions from 1 G Ω down to 100 Ω could be measured. The spectroscopy measurement consists typically of 50-ms voltage sweeps applied between the STM tip and the sample. Faster scans are limited by the frequency cutoff of the converter (around 2 kHz). The stability of the corresponding $I(U)$ curve is checked on an oscilloscope before recording. The data presented in this paper correspond to the average of about 100 $I(U)$ curves taken subsequently at the same point and in the same conditions. We have checked that this averaging process limits the high-frequency noise without affecting the shape of the curves. The tunneling conductance $G(U) = dI/dU$ is finally obtained by numerical differentiation of the averaged $I(U)$ curves.

2. Studied samples

We have measured several samples of the icosahedral AlPdMn, AlCuFe, and AlPdRe alloys.

In the i -AlCuFe system, we have measured polycrystalline ribbons and thin films produced in our laboratory. The ribbons were melt spun¹⁴ at a nominal composition $\text{Al}_{62.7}\text{Cu}_{24.8}\text{Fe}_{12.5}$. After high-temperature annealing ($\approx 800^\circ\text{C}$), the ribbon's resistivity reaches $\approx 10000 \mu\Omega \text{ cm}$ at 4 K and the resistance ratio $\mathcal{R} = 2.3$. Thin films (3000 \AA thick) of nominal composition $\text{Al}_{62.5}\text{Cu}_{25}\text{Fe}_{12.5}$ were obtained by annealing (at 600°C) stacks of sequentially evaporated pure elements.³⁸ This results in high structural quality and homogeneous samples of resistivity around 2000 $\mu\Omega \text{ cm}$ at 4 K and resistance ratio $\mathcal{R} = \rho_{4K} / \rho_{300K}$ around 1.5.

The i -AlPdRe samples are also melt-spun ribbons.^{39,40} For a nominal composition of $\text{Al}_{70.5}\text{Pd}_{21}\text{Re}_{8.5}$ and after annealing up to high temperatures (between 950 and 1000°C), highly resistive samples were obtained. The ribbons chosen in the present tunneling spectroscopy experiment have resistivity

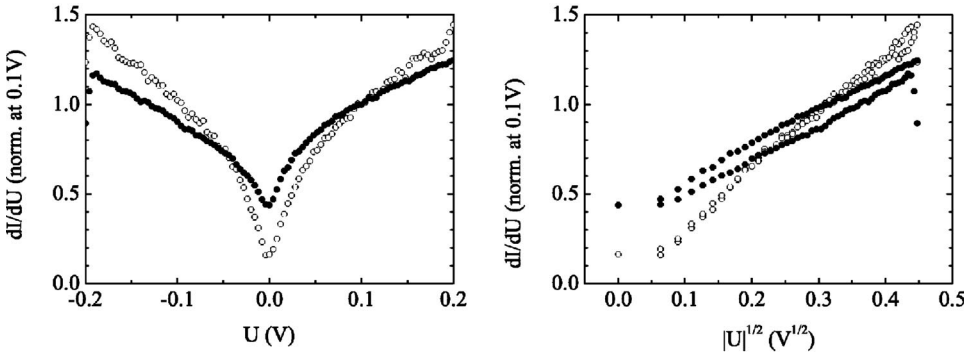


FIG. 1. Normalized tunneling conductance $G(U)=dI/dU$ as a function of U (left panel) and as a function of $\sqrt{|U|}$ (right panel) for an i -AIPdRe polished ribbon. Open symbols, $R_{tunnel}(+0.1V) = 170 \text{ M}\Omega$; closed symbols, other STM tip locations and $R_{tunnel}(+0.1V) = 620 \text{ M}\Omega$.

values $\rho_{4K} \approx 1 \Omega \text{ cm}$ and resistance ratios above 100. According to conductivity measurements,² these ribbons are believed to be zero-temperature insulators.

Some i -AlCuFe and i -AIPdRe ribbon samples were also studied after polishing with a $1\text{-}\mu\text{m}$ diamond paste. The main purpose of this treatment was to flatten the surface to ease the measurement with a STM tip. Note that polishing was reported to induce surface disorder in i -AIPdMn single grains,⁴¹ but this conclusion was derived from a diffraction peak change that could also be ascribed to composition effects in that particular sample. In i -AIPdRe, polishing could also remove the low fraction of residual nonpercolating secondary phases occasionally observed by scanning electron microscope at the surface.⁴⁰ In similar i -AIPdRe samples, the resistance ratio was observed to be somewhat reduced by polishing, probably related to chemical nonhomogeneity within the i phase.⁴² The typical grain size in all the polycrystalline samples is of a few micrometers.

In the i -AIPdMn system, we have measured a single grain.⁴³ The single grain of measured composition $\text{Al}_{70.1}\text{Pd}_{20.4}\text{Mn}_{9.5}$ was pulled out from the melt by the Czochralski method and subsequently homogenized for 120 h at 780°C . A slice was cut perpendicular to a five-fold axis and polished using a $1\text{-}\mu\text{m}$ diamond paste. For this sample, the bulk resistivity is about $\rho_{300K} \approx 1000 \Omega \text{ cm}$ and the resistance ratio around 1.2. The surface was carefully prepared and characterized under UHV. Cycles of ion sputtering and ther-

mal annealing above 60°C were performed, until a fivefold symmetry low-energy electron-diffraction (LEED) pattern was observed, which is the signature of a QC order up to the surface. Indeed, several surface studies have come to the conclusion that such a prepared surface is simply a cut from the bulk.⁴⁴ The single grain was then oxidized under a clean oxygen atmosphere, and measured as soon as possible thereafter.

For each measurement, the sample loaded microscope was sealed in a brass box that was pumped out at room temperature. A low pressure of clean helium was then introduced before cooling.

III. OVERVIEW OF THE RESULTS

A. Typical tunneling spectra

The tunneling spectra $G(U)$ present two general features. First, zero-bias anomalies (i.e., nonlinear I vs U) are present in almost all the $I(U)$ curves. Second, different spectral shapes have been observed, and the deviation from standard metallic linearity is more or less pronounced, depending primarily on the location of the STM tip on the surface. This large range of behavior was observed on each sample, whatever the alloy and the nature of the sample (thin film, ribbon, or single grain). Some ribbons were polished, but this additional step does not change the results significantly. It only gives more stable spectra. We have sorted the tunneling spectra according to their similarities. The most typical examples are reported in Figs. 1–4.

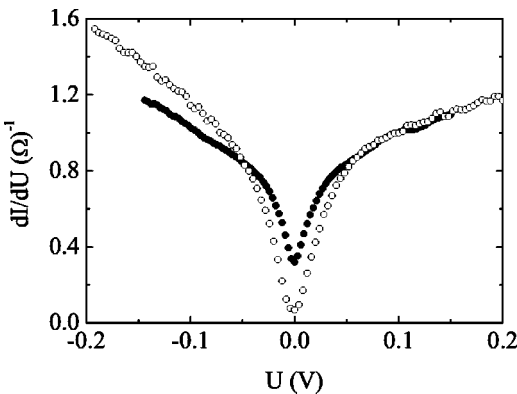


FIG. 2. Normalized tunneling conductance $G(U)=dI/dU$. Open symbols: i -AIPdRe polished ribbon with $R_{tunnel}(+0.1 \text{ V}) = 130 \text{ M}\Omega$. Full symbols: i -AlCuFe polished ribbon with $R_{tunnel}(+0.1 \text{ V}) = 5 \text{ M}\Omega$.

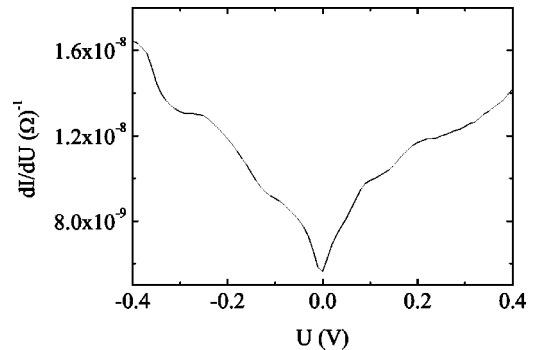


FIG. 3. Tunneling conductance $G(U)=dI/dU$ on an i -AIPdRe ribbon.

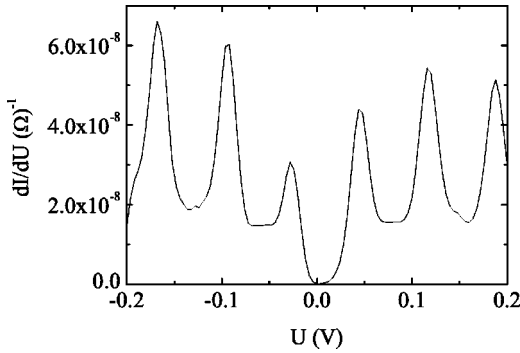


FIG. 4. Tunneling conductance $G(U) = dI/dU$ of an *i*-AlCuFe thin film.

Most of the spectra exhibit a one-dip feature centered at zero bias such as in Figs. 1–3. They are usually well described by a square-root voltage dependence around zero bias, i.e.,

$$G(U) = dI/dU = a + b\sqrt{|U|}. \quad (5)$$

We believe that this law reflects the property of the QC samples themselves, as explained later. The dip can be more or less pronounced and symmetrical, as illustrated in Fig. 1 for *i*-AlPdRe.

In Fig. 2, we can see a symmetrical dip, with a change in the voltage slope around ± 50 mV. In Fig. 3, a dip is also present, but with smooth steps at higher voltage. Combinations of these behaviors and curves less symmetrical were also observed.

We have also observed scarce $I(U)$ spectra with many singularities such as in Fig. 4. The tunneling conductance $G(U) = dI/dU$ is almost suppressed at zero bias and displays a set of sharp peaks periodically spaced in voltage.

Very often, a change in the voltage dependence is observed at high voltages. For example, in Fig. 5, the tunneling conductance is square-root-like for $|U| < 0.2$ V, and parabolic-like elsewhere. For all spectra, a rounded shape is always observed for voltage below ≈ 5 mV, which is 5 times larger than the thermal broadening effects expected at 4 K from relation (2). We believe that this last feature comes from high-frequency noise and does not reflect an actual

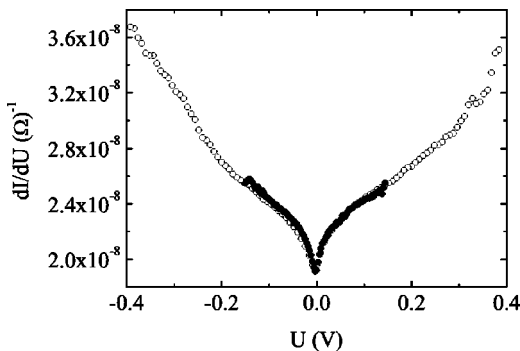


FIG. 5. Tunneling conductance $G(U) = dI/dU$ on a polished *i*-AlCuFe ribbon. The two sets of points are measured at the same STM tip position.

property of the samples. The voltage range below 5 mV is therefore not taken into account in the following analysis.

B. Determination of the intrinsic spectra

Because of this large set of behavior, observed even within one sample, the determination of the intrinsic tunneling spectra requires a close scrutiny. Similar variations were also reported in scanning tunneling studies on high- T_C superconductors.^{45,46} But in this case, the energy dependence of the one-electron DOS was known, at least qualitatively (BCS-like), and allows one to analyze only the tunneling spectra reflecting superconductivity related features. In our experiment, the problem is precisely that the characteristic tunneling spectrum of icosahedral alloys is a fully open question. We thus have performed complementary measurements described below to discriminate between intrinsic and extrinsic effects.

1. Non-quasicrystalline samples

We have measured tunneling spectra of aluminum and gold samples. Al is especially interesting because the bulk electronic properties are quite different from the icosahedral phases, but the surface oxide is believed to be similar on both materials. For the Al samples, no such spectrum as in Fig. 1 could be reproduced, either for bulk or thin-film samples. However, for some locations of the STM tip, we found spectra similar to Figs. 3 and 4. On a gold sample, a much shallower zero-bias anomaly was also sometimes observed.

This indicates that features as in Figs. 3 and 4 have something to do with the Al-based oxide layer and that no all anomalies measured on icosahedral samples reflect a specificity of the bulk electronic structure of icosahedral phase. Possible physical explanations are proposed in the following section.

2. *i*-AlPdMn single grain prepared under UHV

The measurement of the *i*-AlPdMn single grain prepared under UHV and oxidized in a controlled atmosphere of oxygen allowed us to further discriminate between the spectra. As mentioned above, the LEED pattern exhibited a fivefold symmetry before the oxidation stage, which is the signature of a QC order at the surface. The sample was mounted on the STM inside a nitrogen atmosphere box and cooled down as fast as possible. This procedure should give the best surface, in terms of cleanness, structural order, and chemical homogeneity for both the oxide and the atomic layers underneath. Significantly, the tunneling conductance curves are more alike for different tip locations on the surface, and sharp peaks such as those in Fig. 4 have not been found (which, strictly speaking, only proves that they are scarce). Typical curves measured on this sample are presented in Fig. 6 between -0.3 V and $+0.3$ V. As shown by the full line fit, the voltage dependence is well described by the square root law (5), with two examples of characteristic energies $e(a/b)^2 = 380$ meV and 30 meV, respectively.

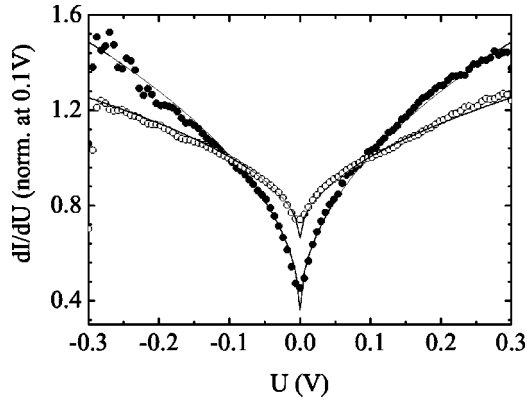


FIG. 6. Tunneling conductance $G(U) = dI/dU$ of the i -AlPdMn single grain prepared under UHV and oxidized under a controlled atmosphere. The two sets of curves correspond to two different locations of the STM tip on the surface. Open symbols, $R_{\text{tunnel}}(+0.1 \text{ V}) = 13 \text{ M}\Omega$; closed symbols, $R_{\text{tunnel}}(+0.1 \text{ V}) = 340 \text{ M}\Omega$. Continuous lines, fits with law (5); fit of the open symbols curve, $0.664 + 1.07\sqrt{|U|}$, $(a/b)^2 = 380 \text{ mV}$; fit of the closed symbols curve, $0.361 + 2.06\sqrt{|U|}$, $(a/b)^2 = 30 \text{ mV}$.

3. Low-resistance junction

Concluding results were also obtained on an i -AlPdRe ribbon. We have reduced the tunneling resistance from $\approx 1 \text{ M}\Omega$ down to $\approx 500 \Omega$, while the x - y location of the STM tip was kept unchanged. As the resistance is lowered, the tip comes very close to the surface and eventually is pushed inside the sample. Indeed, after the measurement, we could see by optical microscopy the deformation of the tip. Thus, at low resistances (of the order of $1 \text{ k}\Omega$), the experiment may be very similar to a planar junction configuration. Then, we can also wonder that to what extent our experiment is still a classical tunneling experiment described by Eqs. (1) and (2), and not a point-contact measurement. But as it is explained below, it seems that even at resistances as low as 500Ω , we still have a tunneling contribution to the current. The resulting curves are presented in Figs. 7–9 for three different junction resistances and different voltage ranges.

At $R = 900 \text{ k}\Omega$ (see Fig. 7), the tunneling spectrum displays a strong singularity at zero bias: the conductance at 0 V is reduced to 5% of its value at 0.3 V . The spectrum is not symmetrical and smooth oscillations are present for positive voltages.

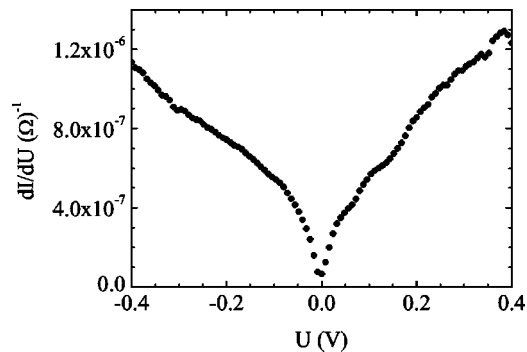


FIG. 7. Tunneling conductance $G(U) = dI/dU$ of a nonpolished i -AlPdRe ribbon, with a junction resistance of $900 \text{ k}\Omega$.

At $R = 2.9 \text{ k}\Omega$ (see Fig. 8), the tunneling spectrum is quite different. The curve is parabolic at high voltages and square-root-like around zero bias ($|U| > 5 \text{ meV}$). The inflexion points are located around $\pm 0.2 \text{ V}$. In tunneling spectroscopy measurements, a parabolic dependence is well known to arise from a decrease of the effective barrier height at high-voltage bias. The slight asymmetry vs bias, polarity may reflect an asymmetry of the tunneling barrier itself. So at high bias this parabolic dependence indicates that the tunneling spectrum is dominated by barrier effects and relations (1) and (2) should not apply. Note that the presence of a high bias parabolic dependence indicates that even for $R = 2.9 \text{ k}\Omega$, there is still a tunneling contribution to the current. At low bias, barrier effects are expected to become negligible and so relation (1) should be valid. Actually for $|U| < \approx 0.1 \text{ V}$ a square root-law-like equation (5) describes accurately the voltage dependence.

For lower junction resistance ($R = 550 \Omega$, see Fig. 9), the parabolic shape is even more visible, due to a reduction of the effective barrier height, and contributes significantly to the tunneling conductance voltage dependence down to the resolution of the experiment ($\approx 5 \text{ mV}$). The curve now appears linear in the window -80 mV and $+80 \text{ mV}$. Interestingly by subtracting a parabolic dependence estimated in the high-voltage range, we find again the square-root law (5) in the resulting tunneling conductance.

The same analysis performed for different junction resistances yields significantly different characteristic energies $e(a/b)^2$ (140 meV when $R = 2.9 \text{ k}\Omega$ and 2.5 eV when $R = 500 \Omega$). We believe that this is due to a nontunneling contribution to the current, relative part of which becomes more and more important when the resistance of the junction is lowered.

In conclusion, the results obtained on crystalline samples, on the well-defined i -AlPdMn surface, and by reducing the resistance junction lead us to consider the square root anomaly as an intrinsic property of the Al-based icosahedral samples. In the next two sections, we present an interpretation of both the extrinsic curves and the square-root anomaly.

IV. INTERPRETATION OF THE RESULTS: EXTRINSIC EFFECTS

Let us focus first on the extrinsic zero-bias anomalies (non-square-root-like). Because these have also been measured on Al surfaces (and even on gold, although less clearly), they cannot be the representative of the bulk i samples. We show in this section that these anomalies can be well understood, at least qualitatively, by considering the Coulomb blockade phenomena.⁴⁷

Any tunnel junction has a capacity C and the change in electrostatic energy associated with the tunneling of one-electron across the junction is given by

$$E_{\text{after}} - E_{\text{before}} = \frac{(Q-e)^2}{2C} - \frac{Q^2}{2C} = \frac{e}{2C}(e-2Q). \quad (6)$$

At zero temperature, tunneling can only occur when this energy is negative, i.e., when the charge Q on the electrodes

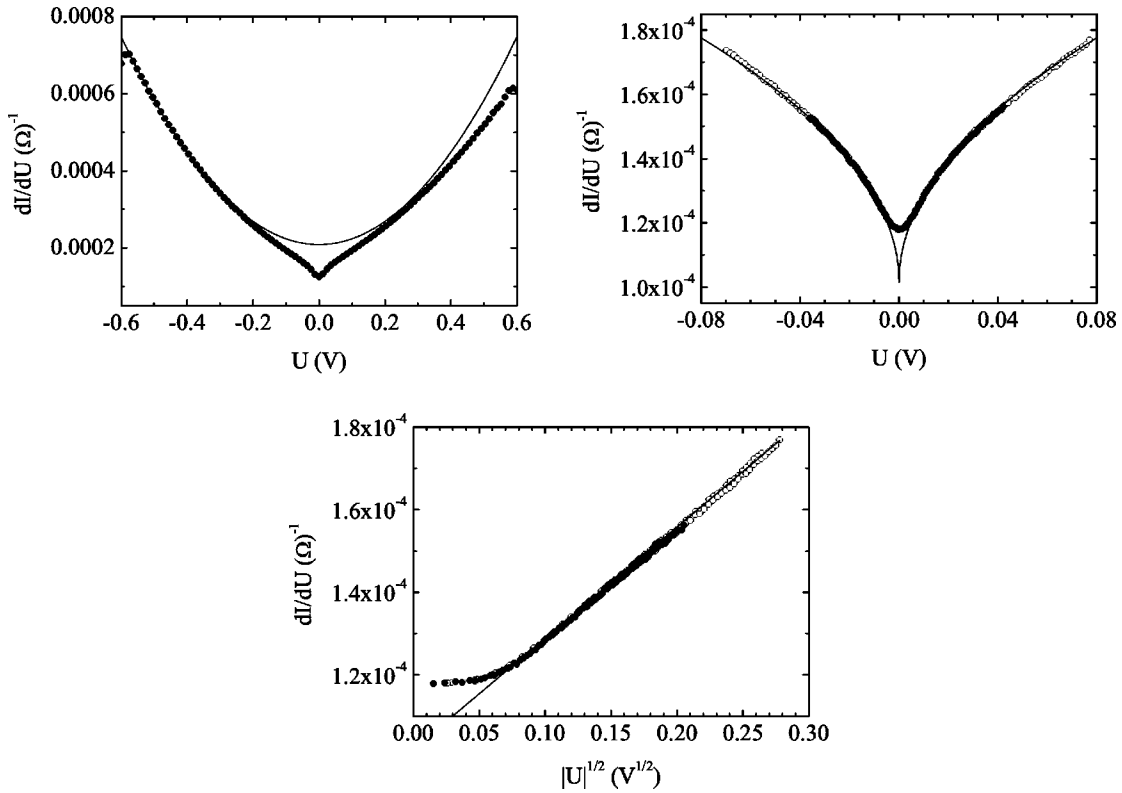


FIG. 8. Tunneling conductance $G(U)=dI/dU$ of the same ribbon i -AlPdRe than Fig. 7 and at the same STM tip position, but with a junction resistance of $2.9\text{ k}\Omega$. Top panel: -0.6 V and $+0.6\text{ V}$ range measurement, with the parabolic dependence fit (continuous line). Lower panel, left: -80 mV and $+80\text{ mV}$ range measurement, and the square-root fit (continuous line) $1.02\times 10^{-4}+2.69\times 10^{-4}\sqrt{|U|}$ and right panel, the tunneling conductance and the square-root fit between -80 mV and $+80\text{ mV}$ as a function of $\sqrt{|U|}$.

before tunneling is larger than $e/2$. If the junction is supplied with a voltage source, tunneling is only possible once the voltage across the junction exceeds $e/2C$. In order to observe clearly these effects, the thermal energy $k_B T$ must be below the charging energy $E_C=e^2/(2C)$, even if charging effects can remain visible by an order of magnitude higher in temperature. In our experiment, assuming an area for the junction of typically a few nanometers, and a separation between the STM tip and the sample of few angstroms, we get a

capacity value of the order of 10^{-18} F . The charging energy corresponds to a temperature of 400 K , 100 times the actual temperature.

However, something must have been misunderstood by describing tunneling by Eq. (6), otherwise no DOS measurements could be achieved to the Fermi level and at low temperature with a STM tip. Indeed, by writing relation (6), we have assumed that the charge was a well-defined (nonfluctuating) quantity in the problem, and that there was no relax-

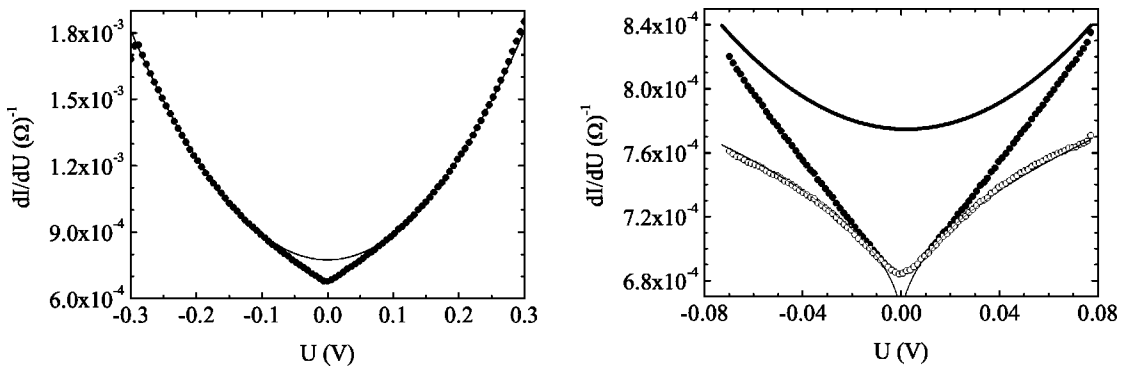


FIG. 9. Tunneling conductance $G(U)=dI/dU$ on the same ribbon i -AlPdRe than on Figs. 7 and 8 and at the same STM tip location but with a junction resistance of $550\ \Omega$. Left panel: -0.3 V and $+0.3\text{ V}$ range measurement, with the parabolic background fit (continuous line). Right panel: -80 mV and $+80\text{ mV}$ range measurement (closed symbols), the parabolic background (thick continuous line), measurement with the parabolic background subtracted (open symbols) and the square-root law fit (thin continuous line) $6.54\times 10^{-4}+4.11\times 10^{-4}\sqrt{|U|}$.

ation of the charge during the tunneling event. These two assumptions are, in fact, related to each other through the fluctuation-dissipation theorem. This is, of course, not always a good description of reality. For instance, let us assume that the junction is supplied with a perfect voltage source, i.e., a source with a zero internal impedance. In this case, the charge on the electrodes is unchanged during a tunneling event, since it is compensated instantaneously at any time by the voltage source. There obviously cannot be a zero-bias anomaly.

In realistic cases, the junction is never supplied by a perfect voltage source. We have to consider the environment of the junction characterized by an impedance $Z(\omega) \neq 0$ and in series with the tunnel junction. This problem has been solved theoretically by the so-called $P(E)$ theory.⁴⁸ Tunneling electrons have a certain probability $P(E)$ to lose the energy E in the environment (i.e., inelastic tunneling is taken into account). The function $P(E)$ can be expressed as a function of $Z(\omega)$ and the capacity C of the junction itself.

Different specific tunneling spectra can be obtained. For instance, if the environment of the junction is a pure inductance (which is so if there is a molecule in the junction, for instance), the tunneling conductance is given by

$$\frac{dI}{dU} = \frac{1}{R_T} \exp(-\rho) \sum_{k=0}^n \frac{\rho^k}{k!}. \quad (7)$$

n is the largest integer smaller or equal to $eU/\hbar\omega_s$, and ρ is a constant equal to $E_C/\hbar\omega_s$ ($\hbar\omega_s = 1/\sqrt{LC}$). The prefactor $\exp(-\rho)$ gives the reduction of the tunneling conductance at zero-bias compared to the limit at large voltages ($1/R_T$). So, a zero-bias anomaly is present in this case only if ρ is large, which means if $E_C \gg \hbar\omega_s$. The $G(U)$ curve is characterized by the presence of steps periodically spaced in voltage (with the period $\hbar\omega_s/e$) and whose amplitude decreases at high voltage. Each time n is increased by 1, electrons can tunnel through the junction via the excitation of one new harmonic in the environment: the tunneling probability and thus the tunneling conductance are increased. The curve takes its minimum value at zero-bias, and recovers at large voltage the usual tunneling conductance $1/R_T$. At finite temperature, the steps are blurred out on the thermal energy scale $k_B T$.

Let us consider now an ideal ohmic impedance R_{ext} . In the limit $R_{ext} = 0$ (perfect voltage source), the electrons cannot lose energy when they tunnel through the junction, and we recover the usual relation $R_T = dU/dI$. In the limit $R_{ext} = \infty$ (perfect current source), electrons always lose the energy E_C and, therefore, the $I(U)$ characteristic is given (for $U > 0$) by

$$I(U) = \frac{eU - E_C}{eR_T} \theta(eU - E_C), \quad (8)$$

where θ is the unit step function. For intermediate resistances, a zero-bias anomaly is present, whose analytic form depends on the ratio $g = R_K/R_{ext}$, where R_K is the quantum of resistance ($R_K = \hbar/e^2 = 26 \text{ k}\Omega$). In particular, the tunneling conductance at a small voltage⁴⁹ is proportional to $|U|^{2/g}$. This relation is actually valid for any kind of environment

with a zero-frequency impedance R_{ext} . At large voltages, the tunneling current must approach the asymptotic curve $(1/R_T)(U - e/2C)$.

We underline that only the resistances located close to the junction (typically few micrometers or less) can lead to such anomalies, since the effective capacity of the junction takes into account all the conducting leads between the tunnel junction and the resistance. If the resistance is far away, then the effective capacity is strongly increased and the charging energy is no longer observable.

If we consider more general situations, for example, a single-mode environment with a finite quality factor, the $G(U)$ curves will show a complex behavior, intermediate between the situations described above, with both steps and power laws around zero-bias.

Within the framework of the $P(E)$ theory, we propose an explanation for the slope changes in the tunneling spectra of Figs. 2 and 3. The singularities of Fig. 2 may be due to the presence of an Ohmic resistance of the order of R_K close to the tunnel junction, which may explain the almost linear dependence at low bias; whereas in Fig. 3, Ohmic and inductive elements located close to the tunnel junction could lead to the singularity and the smooth steps observed around zero-bias.

The inductive part may come from molecules adsorbed at the surface, such as condensed water and organic molecules. The Ohmic contribution may result from a bad electrical contact between the bulk and a grain of the material below the STM tip. In this case, we naturally expect a strong variation from one position of the STM tip to another, even at the nanometer scale. We also expect these zero-bias anomalies to be very similar on icosahedral alloys and on Al, since the energy dependence of the density of states has only a minor influence on the tunneling spectra. Finally, we expect these anomalies to be less present on the single grain prepared under UHV, as it was observed in our measurement.

The spectrum of Fig. 4 is clearly the manifestation of Coulomb blockade phenomena, called incremental charging staircase.⁵⁰ This specific set of peaks appears in the tunneling conductance when a metallic island is connected to a voltage source via two asymmetrical tunnel junctions of capacitance C_1 and C_2 , respectively. In this case, the charge on the island is a well-defined number, multiple of the elementary charge e . Thus, the energy cost to inject a charge on the island is $e^2/2(C_1 + C_2)$, which gives a vanishing tunneling conductance for $|U| < e/(C_1 + C_2)$. It has been shown⁵⁰ that if the junctions are asymmetric (for example, $R_{T_2} \gg R_{T_1}$), peaks arise each time the voltage is increased by the quantity e/C_2 . In our experiment, this situation can be realized if some metallic grains are present on top of the oxide layer or, alternatively, below the oxide but decoupled by a tunneling barrier from the bulk of the sample. We get from Fig. 4, $\approx 70 \text{ mV}$ between the voltage peaks, which corresponds to a capacity C_2 of $\approx 2 \times 10^{-18} \text{ F}$, in good agreement with the previous capacity estimate between the STM tip and the surface. We could also have more than one tunnel junction between the metallic island and the bulk sample resulting in even more complex tunneling spectra. This interpretation seems realistic only for polycrystalline samples or single grains not prepared

under UHV. This is confirmed by the fact that we did not find this kind of anomaly in the single-grain sample prepared under UHV.

Note that the Coulomb blockade effects have been reported in various STS experiments. The incremental charging of metallic grains was clearly identified in materials with nanometer size grains embedded in an insulating matrix,^{51–53} but also in materials where no grains were *a priori* present, for example, high-temperature superconductor oxides^{51,46} or even gold samples.⁵⁴ In this case, explanations such as precipitates or molecules adsorbed on the surface have been proposed. Zero-bias anomalies, very similar to that of Fig. 2 have also been reported, although the results were not always discussed in the light of the $P(E)$ theory. They seem to be favored by the presence of an oxide layer in the tunnel junction on the sample or (and) on the STM tip.⁵⁵

V. INTERPRETATION OF THE RESULTS: INTRINSIC EFFECTS

The charging effects discussed so far cannot explain the square-root voltage dependence observed in the tunneling spectra of the QC samples. We will, therefore, now consider the situation where the tunneling spectra reflect the one-electron density of states, with no Coulomb blockade phenomena (perfect voltage source, $g = R_K/R_{ext} \gg 1$, large capacity). In fact, several models predict a square-root energy dependence on a multiple peak DOS, such as Van Hove singularities or even specific QC models.⁵⁶ We will describe in the following the singularity predicted by Altshuler and Aronov⁵⁷ (AA) and measured in three-dimensional (3D) disordered metals, which we will argue to be relevant in our experiment.

A. One electron versus thermodynamic DOS

One point should be clarified even for an intrinsic tunneling spectrum: what is the relation between the tunneling conductance and the electronic DOS? In other words, which DOS is measured in a tunneling spectroscopy experiment? In fact, we now discuss which physics is hidden behind the simple relation (1) in a non-Coulomb blockade situation.

A tunneling spectroscopy experiment comprises injecting electrons from a metallic electrode into the system of interest. At zero temperature, electrons can only be injected above E_F . The available energy levels E_i 's correspond to the energetic cost of adding one more electron in the system. The number of such states of energy E in a volume unity is, by definition, the one-electron or tunneling DOS ($1e$ -DOS), and is noted down $N(E)$. It is clear from this definition that the $1e$ -DOS may depend on the initial state of the system, and thus it is assumed that the system lies in its fundamental state (minimum total energy) before each electron injection and stays in this configuration during the tunneling time.

This DOS should be differentiated from the thermodynamic DOS, which enters, for example, in the dc conductivity or specific-heat expressions. If a system of N electrons is described by a Hamiltonian H of eigenenergies E_I 's, the thermodynamic DOS is the number of states I of energy E in a

volume unity. In a noninteracting electron system, the two DOS's are the same, but this is not the case when interactions between electrons are taken into account.

This property has been clearly illustrated by Pollak⁵⁸ with the example of an Anderson insulator, where a system of N electrons are exponentially localized by disorder on sites i . Let us assume that an electron is injected on the nearest level E_i above the Fermi level. The new system of $(N+1)$ electrons is no longer in its fundamental state: there is an excess of electrostatic energy around the new electron. The other electrons will reorganize to minimize the total energy of the system due to a hopping term between adjacent sites. In other words, the system lies in an excited state after the injection of the electron, and will relax to its new fundamental state corresponding to $(N+1)$ electrons. This also means that the electron must have been injected at an energy E_{rel} above the Fermi level, which gives rise in the $1e$ -DOS to the Coulomb gap (the Fermi level of N electrons is equal to that of $N+1$ electrons when N is large). In a tunneling experiment, the system is connected to an electron reservoir at a fixed chemical potential, to which a charge e will eventually be transferred to keep the electroneutrality, this charge transfer being not quantified.

For relations (1) and (2) to be valid, the system has to fulfill some requirements. First, the tunneling time, i.e., the time spent by the tunneling electron in the barrier has to be short compared with the relaxation time of the system. Second, the relaxation time has to be short compared with the injection rate of the tunneling electrons. This last requirement guarantees that the system is always in its fundamental state before each injection of a new electron. This is not always the case, especially in disordered insulators where experiments and calculations have shown that the relaxation time can be very long due to disorder and electron-electron interaction effects.⁵⁹ The relaxation time increases with the strength of the disorder and the density of electrons. More precisely, the first transitions toward the fundamental state are very fast, but low-energy transitions associated with long-range electron rearrangements can be arbitrarily long.

The present highly resistive icosahedral alloys share many electronic properties with disordered systems, but have resistivity orders of magnitude lower than the samples where slow relaxation effects have been observed. Thus, we can reasonably consider that this is not an issue in our experiment. Finally, we also assume that the metallic tip and the QC surface do not interact with one another, and that the screening in the QC is therefore not too modified by the metallic electrode.

We will consider in the following that the square-root voltage dependence of the tunneling conductance observed in our QC samples reflects directly the $1e$ -DOS according to relation (1). This means that we have, for $|E| > 5$ meV,

$$N(E) = N(0) + N_1 \sqrt{|E|}, \quad (9)$$

E_F being chosen as the origin of the energies ($E = E_F = 0$).

B. 1e-DOS of disordered systems

In order to understand the square-root energy dependence, we start with the results given for disordered systems on both sides of the Mott-Anderson MI transition.⁶⁰ Indeed, law (9) has been widely observed in the 1e-DOS around E_F for disordered systems on the metallic side of the MI transition. The physical origin is attributed to the electron-electron interactions in the presence of disorder. In fact, it has been shown that highly resistive icosahedral alloys share many electronic properties with disordered systems, for example, the temperature and magnetic-field dependence of the conductivity at low temperature.^{1,2,12} But the question is still open for the 1e-DOS, although this point has already been discussed previously.⁶¹

1. 1e-DOS of disordered systems: Theory

For most systems, electron-electron interactions only imply a renormalization of the noninteracting 1e-DOS. But, when disorder is present, energy-dependent corrections have to be taken into account around the Fermi level.

a. Metallic side and far from the MI transition. On the metallic side and far from the MI transition, disorder localization effects can be treated by a perturbation theory. AA have shown⁵⁷ that the exchange term in the Hartree-Fock equations gives at zero temperature a singularity in the 1e-DOS centered at E_F following Eq. (9), the smaller is the conductivity, the larger the anomaly is. This singularity has an intrinsic temperature dependence and is blurred out on the energy scale $k_B T$ for $T \neq 0$. A square-root temperature dependence is also predicted for the electrical conductivity at low temperature. The length

$$l_m(E) = \sqrt{\frac{\hbar D}{|E|}} \quad (10)$$

is the length scale of the interactions responsible for the 1e-DOS corrections at the energy $E(E=0=E_F)$. Note that Ingold and Nazarov⁴⁸ have obtained a similar result in a nonperturbative approach. The anomaly is there discussed as an inelastic tunneling effect due to the impedance of the electrode itself.

b. Insulating side and far from the MI transition. On the insulating side and far from the MI transition, the presence of a so-called Coulomb gap was also predicted⁶² in the 1e-DOS. We have discussed above its physical origin by considering the Coulomb glass model. Efros and Shklovskii (ES) have proposed a simple model,⁶³ where they showed that a disordered insulator is stable towards electron-hole excitations only if the sites of energy $|E|$ from E_F are separated by at least the distance

$$l_i(E) = \frac{e^2}{K|E|}, \quad (11)$$

where K is the dielectric constant. Corrections to the 1e-DOS are determined by interactions on this length scale. At the Fermi level ($E=0$), l_i is infinite, which means there is no state at E_F . From this argument, a parabolic energy dependence was obtained at 3D for the 1e-DOS around E_F ,

which was later criticized since it does not take into account multielectron excitations in the definition of the fundamental state.⁵⁸ Such effects should lead to a harder gap at small energies (exponential dependence or power law with an exponent above 2 have been suggested). At high energies, the 1e-DOS recovers the value without interaction. The width of the Coulomb gap depends on the parameters of the system, such as the electronic density and the dielectric constant.

c. Close to the MI transition These works and the scaling theory of the MI transition proposed by Abrahams *et al.*⁶⁴ in the noninteracting case have motivated nonperturbative descriptions for disordered systems close to the MI transition including both localization by disorder and electron-electron interactions. On the metallic side, McMillan has proposed a two-parameter scaling theory,⁶⁵ and recently a similar approach was proposed for the insulating side.⁶⁶ Two fundamental quantities are introduced, a length ξ and an energy $E(\xi) = \Delta$, which are related in the metallic and the insulating phase, respectively, by the relations

$$\Delta_m = \frac{\hbar D \xi}{\xi^2}, \quad (12)$$

$$\Delta_i = \frac{e^2}{K \xi \xi}. \quad (13)$$

ξ is the screening length in the metallic phase, and the localization length in the insulating phase. As the MI transition is approached, ξ goes to infinity and Δ goes to zero.

On length scales smaller than ξ (i.e., energies $|E| > \Delta$), the system is in the critical regime of the MI transition. In this regime, the electronic properties of a metal and an insulator have the same length scale (or energy) dependence. Starting a renormalization at the microscopic length L_0 (of the order of the mean free path), McMillan obtained for the energy dependence of the 1e-DOS the power law

$$N_C(E) = N(E(L_0)) \left(\frac{E}{E_0} \right)^{(3/\eta)-1}. \quad (14)$$

η is an exponent relating the length and the energy scales

$$E(L) = E(L_0) \left(\frac{L_0}{L} \right)^\eta. \quad (15)$$

McMillan predicted that $1 < \eta < 3$.

On length scales larger than ξ (i.e., $|E| < \Delta$), the metallic regime and the insulating regime of the MI transition have distinguishable energy and length dependence. In these regimes, we should recover the AA and ES results obtained far from the MI transition. In the metallic regime, McMillan obtained for the 1e-DOS energy dependence

$$N_m(E) = \frac{N(\Delta_m)}{2} \left[1 + \left(\frac{|E|}{\Delta_m} \right)^{1/2} \right]. \quad (16)$$

Since the temperature dependence of the conductivity in this regime is found to be

$$\sigma(T) \approx \frac{e^2}{\hbar \xi} \left[1 + \left(\frac{k_B T}{\Delta_m} \right)^{1/2} \right], \quad (17)$$

we have from relation (15) an interesting relation between the energy Δ_m and the zero-temperature conductivity

$$\Delta_m \propto \sigma(T=0)^\eta. \quad (18)$$

In the insulating regime, we expect the ES parabolic dependence

$$N_i(E) = N(\Delta_i) \left[\frac{|E|}{\Delta_i} \right]^2. \quad (19)$$

Theoretical arguments have been later proposed⁶⁶ to justify the use of the $1e$ -DOS rather than the thermodynamic DOS in evaluating the screening, this point being criticized.⁶⁰ But as a matter of fact, McMillan's theory seems to describe quite well the experimental results.

2. $1e$ -DOS of disordered systems: Tunneling experiments

Tunneling spectroscopy experiments in a planar junction configuration have been performed in a large variety of systems (granular metals,⁶⁷ doped semiconductors,^{68,66} mixture of semiconductors and metals,^{69–72} oxides,⁷³ etc). Far from the MI transition on the metallic side, the AA theory is in good agreement, qualitatively and quantitatively with experiments. In particular, the role of the interaction length $l_m(E)$ has been clearly demonstrated.⁷³ Far from the MI transition on the insulating side, a large voltage drop develops in the sample itself. Because it may give a nonlinear contribution to the voltage dependence of the tunneling current, it makes any quantitative analysis difficult (especially, for 3D systems). Indeed, up to now, experiments on 3D insulating samples are limited to the vicinity of the transition. The most complete study was performed on doped semiconductor SiB samples on both sides of the MI transition.⁶⁶ A common power law was found for all the samples at high energies, which was attributed to the critical regime of the MI transition. At low energy, the $1e$ -DOS spectra exhibit a square-root anomaly around $E=0$ for metallic samples and a parabolic gap for insulating ones. The closer are the samples to the MI transition, the lower is the crossover energy between the high-energy critical regime and the low-energy metallic (insulating) one. These results are in good agreement with the McMillan theory, and were analyzed in the critical regime by $N(E) \propto |E|^m$, with $m=0.43–0.47$, corresponding to η values of 2.1. Exponents $m=1/2$ and $1/3$ were also reported in previous tunneling experiments,^{69,70} although in this case, the critical regime was not clearly identified. In many experiments on disordered systems,⁶⁰ a value $\eta \approx 2$ was also deduced from the low-temperature conductivity according to relation (18).

C. $1e$ -DOS of i -AlCuFe and i -AlPdMn: Interpretation of the square-root law on the metallic side of the MI transition

To understand our tunneling spectroscopy results, we discuss how these “disordered” models can be adapted to quasicrystalline systems.

1. Theoretical considerations

It has been found theoretically^{29–31} that the spreading length of an electronic wave packet in a quasiperiodic potential evolves with time as

$$L(t) = At^\beta. \quad (20)$$

The exponent β depends on the Hamiltonian parameters and on the energy considered. In principle, β can vary between 0 (localized regime) and 1 (ballistic regime), but values below $1/3$ have not been found in 3D models. We call L_{QC} the microscopic length at the onset of this behavior (i.e., anomalous law can only develop for $L > L_{QC}$, once the electrons can actually “feel” the quasiperiodic potential).

If a small disorder is introduced, we expect to recover at large length scales the usual diffusive law

$$L(t) = \sqrt{Dt}. \quad (21)$$

The crossover between relations (20) and (21) corresponds to a length of the order of the elastic mean free path l (that is to the elastic scattering time τ). Note that, recent numerical simulations³³ have shown in 3D quasiperiodic arrays that the situation might be more complex in the presence of disorder. In particular, for a strong-enough quasiperiodic potential, it has been found that the anomalous diffusion persists even after very long times, but the exponent β is changed. Note also that in principle, β could be energy dependent.

We will assume in the following that $|E| > \hbar/k_B T$ (i.e., $L < L_{in}$, where L_{in} is the inelastic mean free path). In QC samples where disorder is always present (structural or chemical defects), we can thus distinguish two regimes: (a) the quasicrystalline regime, for $L_{QC} < L < l$ or $E_{QC} > |E| > \hbar/\tau$, characterized by relation (20). (b) the diffusive regime, for $L > l$ or $|E| < \hbar/\tau$, characterized by Eq. (21).

Energy and length scales are thus related by a general power law $E(L) \propto L^{-\alpha}$, with an exponent α equal to $1/\beta$ in the QC regime, and 2 in the diffusive regime. Following Eqs. (14) and (15) the energy-dependent corrections to the $1e$ -DOS due to electron-electron interactions therefore depend on the exponent α . We thus expect different laws $N(E)$ for $|E| < \hbar/\tau$ and for $|E| > \hbar/\tau$. Even if the interplay between electron-electron interactions and the anomalous spreading of wave functions in 3D systems has not yet been addressed theoretically, we believe that this crossover energy should exist. McMillan's results can be extended by starting the renormalization process at length L_{QC} . Close enough to the MI transition, i.e., when $\xi > (l, L_{QC})$, we get the following regimes.

(a) A QC regime for $L_{QC} < L < l$ or $E_{QC} > |E| > \hbar/\tau$:

$$E(L) \propto L^{-1/\beta'}. \quad (22)$$

β' is an exponent characteristic of the anomalous spreading that takes into account the partial screening of the Coulomb interaction on lengths smaller than ξ . This gives from Eq. (14)

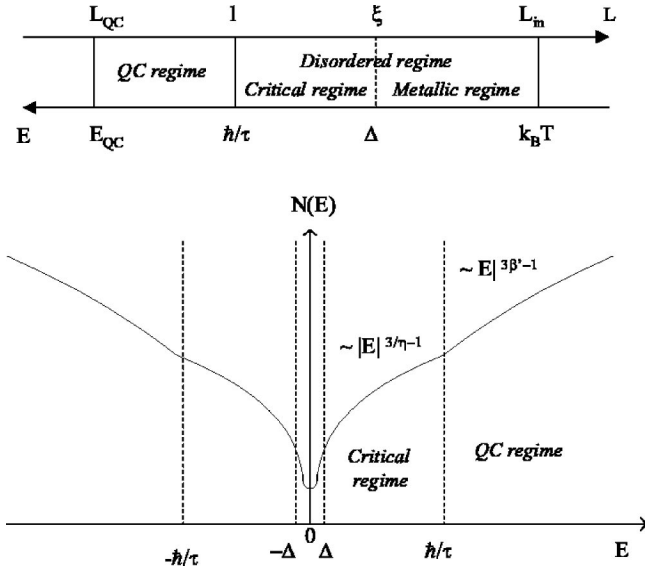


FIG. 10. QC sample close and on the metallic side of the MI transition: energy and length scales, and expected energy dependence of the $1e$ -DOS. The rounded shape around the Fermi level $E=0$ corresponds to thermal effects of width $\sim k_B T$.

$$N(E) = N(E_{QC}) \left(\frac{|E|}{E_{QC}} \right)^{3\beta' - 1}. \quad (23)$$

(b) A disordered critical regime for $l < L < \xi$ or $\hbar/\tau > |E| > \Delta$ characterized by Eq. (14).

(c) A disordered metallic or insulating regime for $L > \xi$ or $|E| < \Delta$, characterized by Eqs. (16) or (19), respectively.

The expected $1e$ -DOS is schematically presented in Fig. 10 for a QC sample on the metallic side of the MI transition.

2. Crossover energy

A realistic estimate of the elastic scattering time τ in highly resistive icosahedral alloys¹⁴ are of the order of 10^{-14} – 10^{-13} s. This corresponds to an energy \hbar/τ between 60 and 6 meV, which falls well in our measurement range. But then, if we believe that tunneling spectra such as Figs. 6 and 8 are the intrinsic spectra of the QC phase, our data give no evidence for a crossover energy in this energy range.

Within the theoretical frame presented above, different reasons could explain an absence of this crossover energy.

(1) The exponent β' may be close or equal to $1/2$. Then, within the experimental precision, the QC and the diffusive regimes cannot be distinguished. Indeed, for many square-root-like spectra, a definitive conclusion is difficult to reach, since a significant uncertainty in the exponent at a given energy remains. For example, in Fig. 6, good fits can be obtained with exponents between 0.5 and 0.6.

(2) The energy \hbar/τ lies above ≈ 100 meV, which means that the scattering time τ is smaller than 10^{-13} s. Then, even if an anomalous regime exists for the $1e$ -DOS, it is out of our measurement range: we only observe the disordered regime (critical or metallic). Let us estimate the associated elastic scattering length. In i -AlCuFe thin films, the diffusion

coefficient has been estimated³⁸ as low as $0.1 \text{ cm}^2 \text{ s}^{-1}$. In this case, according to relation (10), the energy-length correspondence is for $E=1$ eV (100 meV, 10 meV), $L=1$ Å (3 Å, 10 Å, respectively). We believe that the diffusion coefficient is of the same order of magnitude in our i -AlPdMn sample, since the measured transport properties of the two systems are similar. A crossover voltage above 100 meV implies a mean free path smaller than a few angstroms, which is obviously too small to allow for the setting up of an anomalous regime.

(3) The tunneling conductance reflects the properties of a disordered layer present below the oxide, at the surface of the quasicrystalline samples. This has already been discussed in Ref. 25. Indeed, a STM probes the local DOS at the position of the tip. But from previous energy-length scale discussion, the local DOS at energy E is determined by interactions on the length $l(E) = \sqrt{\hbar D / |E|}$. The smaller is the bias voltage, the more the tunneling spectra reflects the bulk. This hypothesis can be relevant for some samples, such as ribbons or thin films that can have disordered grain boundaries or occasionally a scarce secondary phase. But it seems unlikely for the i -AlPdMn single grain which has been prepared under UHV and with a well characterized surface order. It cannot be ruled out, however, that after oxidation, the composition close to the surface is slightly different from the volume.

Without either the accurate knowledge of the elastic scattering time for each sample or the precise structural quality and composition a few layers below the oxide, we cannot decide between the three hypotheses.

3. Magnitude of the $N(E)$ anomaly

We discuss here the magnitude of the square-root anomaly, i.e., the values of the characteristic parameter Δ . In disordered systems, Δ measures the proximity to the MI transition, the smaller Δ is, the closer the system is to the transition. A rough estimate of this energy can be read directly on the $I(U)$ curves since for $|E| = \Delta$, $N(E) = N(0)/2$. As already noticed,²⁵ we have found a large range of Δ values (from ≈ 1 eV down to 1 meV) depending on the STM tip position on the surface. So we can not deduce any reliable average value from such a dispersion. In the case of the single grain i -AlPdMn, where the dispersion was smaller, typical values are around 100 meV (see Fig. 6).

We know from relation (17) that Δ can also be deduced from the low-temperature dependence of the conductivity. This has been done by Lin *et al.*⁷⁴ in a large number of icosahedral alloys (i -AlPdRe, i -AlCuRu, i -AlCuFe, and i -AlPdMn). They found a common relation $\Delta = A \sigma(T=0)^\eta$ for all the samples, with $\eta \approx 2$, which corresponds to the prediction of Eq. (18). Accordingly, Δ should be of the order of 100 meV for our i -AlCuFe samples [$\rho(T=0) \approx 10^{-2} \Omega \text{ cm}$] and 10 eV for our single grain i -AlPdMn [$\rho(T=0) \approx 10^{-3} \Omega \text{ cm}$]. Dynes and Garno⁶⁷ have also correlated Δ extracted from tunneling data and the zero-temperature conductivity but in granular aluminum. This correlation gives similar values of 2 eV for i -AlPdMn and 20 meV for i -AlCuFe.

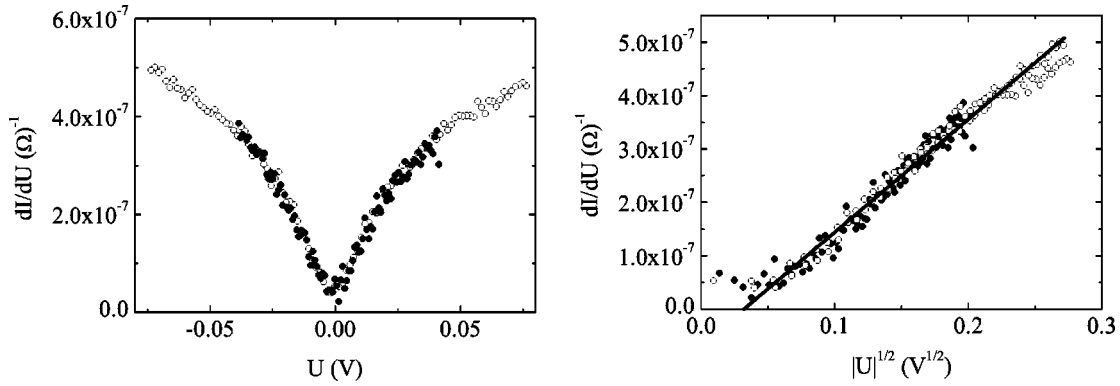


FIG. 11. Tunneling conductance measured on a polished *i*-AlPdRe ribbon and plotted as a function of U (left panel) and $\sqrt{|U|}$ (right panel).

Recent experiments on magnetic properties²⁰ have shown that our *i*-AlPdMn single grain should contain a significant amount of defects, according to its conductivity value. The Mn composition being quite far from the ideal composition, we expect a locally defect-enhanced DOS which could lead to a better conduction. We recall that on these QC's, the more defects there are the better is the conduction. Tunneling through a less defective region might explain the occurrence of Δ values much smaller than the one expected from the bulk conductivity (as low as 30 meV in Fig. 6). Local defects, such as imperfect QC grains, grain boundaries or even secondary phases, might explain the large dispersion in the Δ values of the *i*-AlCuFe polycrystalline samples.

Moreover, photoemission measurements⁷⁵ have been performed on the same *i*-AlPdMn surface at low temperature, but with no oxide layer. The photoemission spectra have also been analyzed by the square-root law (9) between 30 meV and ≈ 500 meV with a parameter Δ around 60 meV, in good agreement with Fig. 6. In this case, the DOS measured is a spatial average value taken on a surface corresponding to the size of the UV beam. Note that the DOS measured in photoemission is the joint density of states which, in principle, may differ from the $1e$ -DOS.⁷⁶

D. $1e$ -DOS of the *i*-AlPdRe ribbons: Insulating side of the MI transition

The *i*-AlPdRe ribbon case is discussed separately because according to their low temperature conductivity, the measured ribbons are on the insulating side of the MI transition. We then expect at low energies the opening of a Coulomb gap in the $1e$ -DOS, as it was observed in disordered insulating systems.⁶⁶

We have indeed found some $G(U)$ curves with a parabolic shape around zero bias which were not found in the other alloys. The width of the gap is ≈ 50 meV, which seems to be extremely large for a Coulomb gap, according to the conductivity value. Indeed, the width of the Coulomb gap depends on the parameters of the system and is very narrow close to the MI transition, with a critical power law at higher energies common with the metallic phase. The presence of a Coulomb gap is associated with a specific activation law $\sigma(T) = \sigma_1 \exp[-(T_{ES}/T)^{1/2}]$ when $k_B T < \approx \Delta_{CG}$ (the Efros

and Shklovskii variable range hopping conductivity). We know from our conductivity measurements² that this law is not observed above 1 K (nor below down to 20 mK) in our ribbons. This should imply that, if there is a Coulomb gap, its energy width Δ_{CG} is far below 0.25 meV, and thus undetectable in our experiment. We cannot rule out that the Coulomb blockade effect is an explanation to these $G(U)$ parabolic spectra.

In our accessible energy range, the $1e$ -DOS then should be the critical power law (14). We have measured on our *i*-AlPdRe ribbons the square-root $G(U)$ spectra following $G(U) = a + b\sqrt{|U|}$ [Eq. (5)]. Although parameters similar to *i*-AlCuFe and *i*-AlPdMn spectra were measured, we have also found spectra with negative a values (Fig. 11). This feature has been identified in disordered systems experiment as the signature of an insulating state.⁷⁰ We emphasize that we have not found negative a values in any *i*-AlPdMn or *i*-AlCuFe samples. Such spectra may therefore be a specificity of the present *i*-AlPdRe samples, which we have characterized to be zero-temperature insulators from conductivity measurements.²

The resistivity at 4 K of our *i*-AlPdRe ribbons spans the range from $1 \Omega \text{ cm}$ down to $10^{-2} \Omega \text{ cm}$, even for ribbons made by the same process and with the same nominal composition.⁴⁰ We believe these variations can reflect a sample-dependent average over electrical nonhomogeneity in the samples. These are indeed expected to arise from the strong sensitivity to composition or structural order, usually observed close to the MI transition. Assuming that these resistivity values reflect the range of local nonhomogeneity, we expect large differences in the $1e$ -DOS parameters at low energies, as observed. For instance, following Lin's correlation,⁷⁴ such resistivity values correspond to $\Delta = 0.1$ meV (10 meV, respectively). However, our measurement does not allow a definite conclusion about the actual nature of the transition.⁷⁷

VI. COMPARISON WITH OTHER TUNNELING SPECTROSCOPY RESULTS

We discuss here our results together with previous reports on tunneling spectroscopy on QC samples. To our knowledge, different techniques have been used at low tempera-

ture: STS (Klein *et al.*²⁴ and Davydov *et al.*²⁵), break junctions (Davydov *et al.*²⁵), and planar junctions (Escudero *et al.*,²⁶ Guohong *et al.*²⁷).

A. Absence of multiple fine structures

The first point is the absence of the multiple sharp peaks and pseudogaps in the tunneling spectra of QC's predicted in the DOS of QC's from *ab initio* calculations. Our tunneling results are in agreement with STS (Refs. 24 and 25) and break junction measurements:²⁴ we have observed a single sharp dip, symmetric and centered at zero-bias. No other peaks or dips are visible in the range -300 mV $+300$ mV. When other structures are observed (such as in Figs. 3 and 4), they are either nonreproducible, or symmetrical around zero-bias and even periodically spaced in voltage. Because of such symmetry, a DOS origin can be ruled out for these spectra since many irregular structures are calculated for the DOS. We have confidently ascribed these spectra to the Coulomb blockade effects (see above Sec. IV).

Similarly, most of the tunneling spectra measured by Escudero *et al.*²⁶ display a single symmetric dip centered at the Fermi level. In one case, an asymmetric feature was measured on an Al/*i*-AlCuFe junction which was ascribed to the predicted fine structure. This spectrum appears only once and was attributed to the tunneling through a perfect QC grain. For our measured spectra locally similar to this one, we think that a more plausible explanation is extrinsic effects (defects in the barrier, localized states, etc.).

Guohong *et al.*²⁷ have ascribed their spectra to the predicted fine structure in low-temperature spectroscopy on an Al/*d*-AlNiCo planar junction. The tunneling spectra display sharp peaks and pseudogaps, but unexpectedly symmetric according to zero-bias. It was shown later²⁸ that these peaks are due to nontrivial superconductivity effects, induced by the presence of the superconducting Al thin-film electrode. Interestingly, at high field, the tunneling spectra exhibit a single dip, symmetric and centered at zero-bias, in agreement with the other studies.

B. Voltage dependence of the tunneling spectra close to E_F

The voltage dependence of the tunneling spectra close to zero-bias appears more controversial.

Klein *et al.* and Davydov *et al.* have reported a square-root voltage dependence at high voltages, which evolves towards a parabolic dependence at low voltages. The concavity change is observed around 30 mV. The energy crossover was tentatively explained²⁵ by using the energy-length scale argument (see Sec. V C: the square-root behavior could reflect the properties of a disordered layer beneath the surface, whereas the parabolic shape would reflect the QC bulk properties).

In the present STS study, we have observed a square-root voltage dependence down to 5 mV. Most probably, the parabolic dependence a few millivolts around zero-bias is due to the noise level of the experiment. It is not clear what is the reason for the discrepancy for the *i*-AlPdRe and *i*-AlCuFe samples measured in both experiments, which were produced in the same laboratory. Also, we have found low-

voltage square-root dependence with high tunneling resistance ($R \approx 100$ M Ω) as well as low values ($R \approx 50$ k Ω) comparable to the study in Ref. 25.

In agreement with our present finding, no clear intrinsic parabolic dependence was found by Escudero *et al.*²⁶ around zero-bias, with a resolution good enough to detect the superconducting gap of Al and In. Typical tunneling spectra display a parabolic dependence at high voltages (100 mV and more) and a square-root dependence at low voltages. A rounded shape is observed only below 1 mV in *i*-AlCuFe alloys, which corresponds to the thermal broadening energy ($T=2$ K). For an *i*-AlPdRe ribbon, the rounded shape extends up to 10 mV, i.e., ten times the value expected from the thermal broadening. This last feature might be due to an *i*-AlPdRe specificity (very high resistivity $\rho_{4K}/\rho_{300K} > 30$ and insulating state). Escudero *et al.* have tentatively fit their data with the square-root law (16) according to AA and McMillan theories, but the fit was found in disagreement with the experimental data. Note that the fit was constrained to take the value $G(U=0, T)$ at zero-bias, although the AA and McMillan models break down at energies of the order of $k_B T$ (and, obviously, below the broadening energy) which may explain the disagreement.

Finally, the tunneling spectra measured by Guohong *et al.*²⁷ at high fields on a less resistive decagonal phase also show a negative concavity (square-root-like) which extend down to 0.5 meV. But no detailed analysis of the voltage dependence was performed.

C. Correlation with the alloy resistivity

The last point to be discussed is the amplitude of the zero-bias anomaly.

Davydov *et al.*²⁵ have estimated that the more resistive the phase is, the deeper is the anomaly. As in our case, it was noted that the values vary considerably from one tunneling contact to another. The Δ parameters extracted from the McMillan law (16) follow the same trend, with Δ of the order of 40 meV for *i*-AlPdRe and 140 meV for *i*-AlCuFe. A qualitative comparison with our results is difficult, since our data are quite spread over and we were not able to deduce a reliable average value. For the *i*-AlPdMn single grain prepared under UHV (not studied by Davydov *et al.*), the fluctuations were smaller and we find a range of values in reasonable agreement (Δ in the range ≈ 30 –380 meV).

Escudero *et al.*²⁶ have noticed a trend in the shape of their tunneling spectra as a function of icosahedral alloys resistivity. For more resistive samples, the parabolic shape starts at higher energies, and the central square-root dip appears wider. The parabolic energy dependence is interpreted as the large DOS pseudogap expected and already measured by other techniques. The tunneling resistances used by Escudero *et al.* range between few 10 Ω and few k Ω . In our experiment, a large parabolic pseudogap also appears at high voltage for such low tunnel resistances. This can be simply explained by a reduction of the tunneling barrier with the junction resistance (see Figs. 8 and 9). Moreover, we have observed that an increase of the tunneling resistance shifts the parabolic dependence towards higher voltage, within the

same sample. Unfortunately, Escudero *et al.* have measured the more resistive samples with the higher tunneling resistances, which forbids any reliable conclusion.

VII. SUMMARY

The first conclusion of this tunneling spectroscopy study on highly resistive icosahedral alloys is that we did not observe the fine structure predicted by LMTO calculations. One possible reason may be that LMTO calculations do not take into account disorder and electron-electron interactions. Indeed, there is a general agreement on this point between all the tunneling experiments performed so far.

The second conclusion is that the quasicrystalline surfaces are characterized by a square-root dip in their $1e$ -DOS. This dip is symmetric, centered at the Fermi level, and the square root energy dependence is followed up to ≈ 300 meV. In analogy with what has been predicted and observed in disordered systems, we naturally expect a square-root singularity in the $1e$ -DOS close to the Fermi level. It comes from the combined effect of electron-electron interactions and disorder. The fact that the square-root energy dependence is observed up to ≈ 100 meV is surprising, since we would have expected an inflexion reflecting the QC specific diffusion laws. It thus appears that the low-energy $1e$ -DOS (referring to the Fermi level), such as the conductivity and magnetoconductivity at low temperatures, is similar to what is observed in disordered systems at proximity of the Mott-Anderson MI transition.

The third conclusion is that spectra with a negative a ($dI/dU = a + b\sqrt{|U|}$) have been measured for i -AlPdRe only. In disordered systems, this feature was observed in insulating samples. However, we have not observed the Efros-Shklovskii parabolic dependence around zero-bias, which might require a much better resolution than the present one.

We have also discussed in this paper the nature of the density of states measured by the scanning spectroscopy technique. For example, the $1e$ -DOS is *a priori* different

from the thermodynamic DOS measured by specific-heat measurements. Similar precautions must be taken when comparing with nuclear-magnetic-resonance or photoemission experiments.

The present analysis also underlines that some caution should be exerted while extracting the intrinsic behavior of the QC alloys. We have found clear signatures of the Coulomb blockade phenomena, such as incremental charging of single grains. Indeed, a poor control of the surface state is one of the major limits of this and previous studies. Tending to a better control, we have performed the first tunneling spectroscopy measurement of an i -AlPdMn single grain with a surface carefully prepared and characterized under UHV. The fluctuations from one location of the STM tip to another on the surface are smaller than for ribbons or thin films. Preparation of quasicrystalline single grains surfaces have been in steady progress recently, especially in the i -AlPdMn and i -AlCuFe alloys. It would be very interesting to perform a scanning tunneling spectroscopy experiment at low temperature under UHV on a bare surface. On the other hand, planar junction measurements with high quality tunneling barrier (no pinholes) could also provide complementary information since fluctuations are naturally averaged in this technique.

Finally, the origin of the high resistivity observed in icosahedral alloys is a recurrent question that is again emphasized in this study. It appears that a complete picture should include not only the quasiperiodicity, but also disorder (always present at large length scales) and electron-electron interactions.

ACKNOWLEDGMENTS

We acknowledge T. Grenet and F. Giroud for kindly providing the i -AlCuFe thin films, and G. Fourcaudot, J. C. Grieco, and C. Gignoux for the i -AlPdRe ribbons. A. G. M. Jansen is also thanked for providing the original STM setup. We are grateful for enlightening discussions with D. Mayou.

*Present address: LCMC-CNRS, Avenue des Martyrs, BP 166 38042 Grenoble Cedex 9, France.

†On sabbatical at GATECH, School of Physics, Atlanta GA30332-0430, USA.

¹T. Grenet, in *Quasicrystals, Current Topics*, edited by E. Belin-Ferré, C. Berger, M. Quiquandon, and A. Sadoc (World Scientific, Singapore, 2000), p. 455, and references therein.

²J. Delahaye, J.P. Brison, and C. Berger, *Phys. Rev. Lett.* **81**, 4204 (1998); J. Delahaye and C. Berger, *Phys. Rev. B* **64**, 094203 (2001)

³E. Belin-Ferré, in *Quasicrystals*, edited by J. M. Dubois, P. A. Thiel, A.-P. Tsai, and K. Urban, MRS Symposia Proceedings No. 553 (Materials Research Society, Pittsburgh, 1999), p. 347.

⁴X. Wu, S.W. Kycia, C.G. Olson, P.J. Benning, A.I. Goldman, and D.W. Lynch, *Phys. Rev. Lett.* **75**, 4540 (1995).

⁵Z.M. Stadnik, D. Purdie, M. Garnier, Y. Baer, A.-P. Tsai, A. Inoue, K. Edagawa, and S. Takeuchi, *Phys. Rev. Lett.* **77**, 1777 (1996).

⁶D. Naumović, P. Aebi, L. Schlapbach, C. Beeli, T.A. Lograsso, and D.W. Delaney, *Phys. Rev. B* **60**, R16330 (1999).

⁷G. Neuhold, S.R. Barman, K. Horn, W. Theis, P. Ebert, and K. Urban, *Phys. Rev. B* **58**, 734 (1998).

⁸C.C. Homes, T. Timusk, X. Wu, Z. Altounian, A. Sahnoune, and J.O. Ström-Olsen, *Phys. Rev. Lett.* **67**, 2694 (1991).

⁹L. Degiorgi, M.A. Chernikov, C. Beeli, and H.R. Ott, *Solid State Commun.* **87**, 721 (1993).

¹⁰A.D. Bianchi, F. Bommeli, M.A. Chernikov, U. Gubler, L. Degiorgi, and H.R. Ott, *Phys. Rev. B* **55**, 5730 (1997).

¹¹U. Mizutani, *J. Phys.: Condens. Matter* **10**, 4609 (1998).

¹²O. Rapp, in *Physical Properties of Quasicrystals*, edited by Z. M. Stadnik, Springer Series in Solid-State Sciences Vol. 126 (Springer, Berlin, 1999), p. 127, and references therein.

¹³J.C. Lasjaunias, A. Sulpice, N. Keller, J.J. Préjean, and M. de Boissieu, *Phys. Rev. B* **52**, 886 (1995).

- ¹⁴T. Klein, C. Berger, D. Mayou, and F. Cyrot-Lackmann, *Phys. Rev. Lett.* **66**, 2907 (1991).
- ¹⁵F.S. Pierce, Q. Guo, and S.J. Poon, *Phys. Rev. Lett.* **73**, 2220 (1994).
- ¹⁶J.J. Préjean, J.C. Lasjaunias, C. Berger, and A. Sulpice, *Phys. Rev. B* **61**, 9356 (2000).
- ¹⁷G. Trambly de Laissardière and T. Fujiwara, *Phys. Rev. B* **50**, 5999 (1994).
- ¹⁸G. Trambly de Laissardière and D. Mayou, *Phys. Rev. B* **55**, 2890 (1997).
- ¹⁹C. Berger, in *Lectures on Quasicrystals*, edited by F. Hippert and D. Gratias (Les Editions de Physique, Les Ulis, 1994) and references therein.
- ²⁰J.J. Préjean, C. Berger, A. Sulpice, and Y. Calvayrac, *Phys. Rev. B* **65**, 140203(R) (2002).
- ²¹E.S. Zijlstra and T. Janssen, *Europhys. Lett.* **52**, 578 (2000).
- ²²F. Giroud, T. Grenet, C. Berger, P. Lindqvist, C. Gignoux, and G. Fourcaudot, *Czech. Phys.* **46-S6**, 2709 (1996); J. Delahaye, C. Berger, T. Grenet, and G. Fourcaudot, in *Quasicrystals*, edited by E. Belin-Ferré, P.A. Thiel, A-P. Tsai, and K. Urban, MRS Symposia Proceedings No. 643 (Materials Research Society, Warrendale, PA, 2001).
- ²³X.-P. Tang, E.A. Hill, S.K. Wonnell, S.J. Poon, and Y. Wu, *Phys. Rev. Lett.* **79**, 1070 (1997); V. Simonet, F. Hippert, C. Gignoux, C. Berger, and Y. Calvayrac, in *Proceedings of the International Conference on Quasicrystals ICQ6 Tokyo, 1997*, edited by S. Takeuchi and T. Fujiwara (World Scientific, Singapore, 1998).
- ²⁴T. Klein, O.G. Symko, D.N. Davydov, and A.G.M. Jansen, *Phys. Rev. Lett.* **74**, 3656 (1995).
- ²⁵D.N. Davydov, D. Mayou, C. Berger, C. Gignoux, A. Neumann, A.G.M. Jansen, and P. Wyder, *Phys. Rev. Lett.* **77**, 3173 (1996).
- ²⁶R. Escudero, J.C. Lasjaunias, Y. Calvayrac, and M. Boudard, *J. Phys.: Condens. Matter* **11**, 383 (1999).
- ²⁷L. Guohong, H. Haifeng, W. Yunping, L. Li, L. Shanlin, J. Xiunian, and Z. Dianlin, *Phys. Rev. Lett.* **82**, 1229 (1999).
- ²⁸C. Berger, D. Mayou, T. Grenet, and Z. Ovadyahu, *Phys. Rev. Lett.* **83**, 3968 (1999).
- ²⁹D. Mayou, in *Quasicrystals, Current Topics*, edited by E. Belin-Ferré, C. Berger, M. Quiquandon, and A. Sadoc (World Scientific, Singapore, 2000), p. 412, and references therein.
- ³⁰T. Fujiwara, in *Physical Properties of Quasicrystals*, Springer Series in Solid-State Sciences Vol. 126, edited by Z. M. Stadnik, (Springer, Berlin, 1999) p. 169, and references therein.
- ³¹B. Passaro, C. Sire, V.G. Benza, *Phys. Rev. B* **46**, 13 751 (1992).
- ³²S. Roche and D. Mayou, *Phys. Rev. Lett.* **79**, 2518 (1997).
- ³³F. Triozon and D. Mayou, *Mater. Sci. Eng., A* **294-296**, 496 (2000).
- ³⁴E. L. Wolf, in *Principles of Electron Tunneling Spectroscopy* (Oxford University Press, New York, 1985).
- ³⁵J. Tersoff and D.R. Hamann, *Phys. Rev. Lett.* **50**, 1998 (1983); J. Tersoff and D.R. Hamann, *Phys. Rev. B* **31**, 805 (1985).
- ³⁶A. Selloni, P. Carnevali, E. Tosatti, and C.D. Chen, *Phys. Rev. B* **31**, 2602 (1985).
- ³⁷N.D. Lang, *Phys. Rev. B* **34**, 5947 (1986).
- ³⁸T. Grenet and F. Giroud, *Eur. Phys. J. B* **23**, 165 (2001).
- ³⁹C. Gignoux, C. Berger, G. Fourcaudot, J.C. Grieco, and H. Rakoto, *Europhys. Lett.* **39**, 171 (1997).
- ⁴⁰J. Delahaye, C. Gignoux, T. Schaub, C. Berger, T. Grenet, A. Sulpice, J.J. Préjean, and J.C. Lasjaunias, *J. Non-Cryst. Solids* **250-252**, 874 (1999).
- ⁴¹M. Boudard, M. de Boissieu, J.P. Simon, J.F. Berar, and B. Doisneau, *Philos. Mag. Lett.* **74**, 429 (1996).
- ⁴²J. Delahaye, C. Berger, and G. Fourcaudot (unpublished).
- ⁴³J. Alvarez, Y. Calvayrac, J.L. Joulaud, and M.J. Capitan, *Surf. Sci.* **423**, L251 (1999).
- ⁴⁴L. Barbier, D. Le Floch, Y. Calvayrac, and D. Gratias, *Phys. Rev. Lett.* **88**, 085506 (2002).
- ⁴⁵P.J.M. van Benthum, H. van Kempen, L.E.C. van de Leemput, and P.A.A. Teunissen, *Phys. Rev. Lett.* **60**, 369 (1988).
- ⁴⁶R. Wilkins, M. Amman, R.E. Soltis, E. Ben-Jacob, and R.C. Jaklevic, *Phys. Rev. B* **41**, 8904 (1990).
- ⁴⁷D.V. Averin and K.K. Likharev, *J. Low Temp. Phys.* **62**, 345 (1986).
- ⁴⁸G.-L. Ingold and Y. V. Nazarov, in *Single Charge Tunneling*, edited by H. Grabert and M. H Devoret (Plenum Press, New York, 1992), p. 21.
- ⁴⁹M.H. Devoret, D. Esteve, H. Grabert, G.-L. Ingold, H. Pothier, and C. Urbina, *Phys. Rev. Lett.* **64**, 1824 (1990).
- ⁵⁰K. Mullen, E. Ben-Jacob, R.C. Jaklevic, and Z. Schuss, *Phys. Rev. B* **37**, 98 (1988).
- ⁵¹P.J.M. van Benthum, R.T.M. Smokers, and H. van Kempen, *Phys. Rev. Lett.* **60**, 2543 (1988).
- ⁵²R. Wilkins, E. Ben-Jacob, and R.C. Jaklevic, *Phys. Rev. Lett.* **63**, 801 (1989).
- ⁵³E. Bar-Sadeh, Y. Goldstein, C. Zhang, H. Deng, B. Abeles, and O. Millo, *Phys. Rev. B* **50**, 8961 (1994).
- ⁵⁴A.E. Hanna and M. Tinkham, *Phys. Rev. B* **44**, 5919 (1991).
- ⁵⁵R. Wilkins, M. Amman, E. Ben-Jacob, and R.C. Jaklevic, *Phys. Rev. B* **42**, 8698 (1990).
- ⁵⁶C. Janot and M. De Boissieu, *Phys. Rev. Lett.* **72**, 1674 (1994).
- ⁵⁷B.L. Altshuler and A.G. Aronov, *Solid State Commun.* **30**, 115 (1979); B. L. Altshuler and A. G. Aronov, in *Electron Electron Interactions in Disordered Systems*, edited by A. L. Efros and M. Pollak (North-Holland, Amsterdam, 1985), p. 1.
- ⁵⁸M. Pollak, *Philos. Mag. B* **65**, 657 (1992).
- ⁵⁹A. Vaknin, Z. Ovadyahuh, and M. Pollak, *Phys. Rev. Lett.* **81**, 669 (1998).
- ⁶⁰D. Belitz and T.R. Kirkpatrick, *Rev. Mod. Phys.* **66**, 261 (1994).
- ⁶¹T. Schaub, J. Delahaye, C. Gignoux, C. Berger, G. Fourcaudot, F. Giroud, T. Grenet, and A.G.M. Jansen, *J. Non-Cryst. Solids* **250-252**, 883 (1999).
- ⁶²M. Pollak, *J. Non-Cryst. Solids* **11**, 1 (1972).
- ⁶³A.L. Efros and B.I. Shklovskii, *J. Phys. C* **8**, L49 (1975); B. I. Shklovskii and A. L. Efros, in *Electronic Properties of Doped Semiconductors*, Springer Series in Solid State Sciences Vol. 45 (Springer-Verlag, Berlin, 1984).
- ⁶⁴E. Abrahams, P.W. Anderson, D.C. Licciardello, and T.V. Ramakrishnan, *Phys. Rev. Lett.* **42**, 673 (1979).
- ⁶⁵W.L. McMillan, *Phys. Rev. B* **24**, 2739 (1981).
- ⁶⁶M. Lee, J.G. Massey, V.L. Nguyen, and B.I. Shklovskii, *Phys. Rev. B* **60**, 1582 (1999).
- ⁶⁷R.C. Dynes and J.P. Garno, *Phys. Rev. Lett.* **46**, 137 (1981).
- ⁶⁸J.G. Massey and M. Lee, *Phys. Rev. Lett.* **77**, 3399 (1996).
- ⁶⁹W.L. McMillan and J. Mochel, *Phys. Rev. Lett.* **46**, 556 (1981).

- ⁷⁰G. Hertel, D.J. Bishop, E.G. Spencer, J.M. Rowell, and R.C. Dynes, *Phys. Rev. Lett.* **50**, 743 (1983).
- ⁷¹J. Lesueur, L. Dumoulin, and P. Nedellec, *Phys. Rev. Lett.* **55**, 2355 (1985).
- ⁷²W. Teizer, F. Hellman, and R.C. Dynes, *Phys. Rev. Lett.* **85**, 848 (2000).
- ⁷³Y. Imry and Z. Ovadyahu, *Phys. Rev. Lett.* **49**, 841 (1982).
- ⁷⁴C.R. Lin, S.L. Chou, and S.T. Lin, *J. Phys.: Condens. Matter* **8**, L725 (1996).
- ⁷⁵T. Schaub, J. Delahaye, C. Berger, H. Guyot, R. Belkhou, A. Taleb-Ibrahimi, and Y. Calvayrac, *Eur. Phys. J. B* **20**, 183 (2001).
- ⁷⁶S. Hufner, *Photoelectron Spectroscopy*, 2nd ed. (Springer-Verlag, Berlin, 1996).
- ⁷⁷I.R. Fisher, X.P. Xie, I. Tudosa, C.W. Gao, C. Song, P.C. Canfield, A. Kracher, K. Dennis, D. Abanoz, and M.J. Kramer, *Philos. Mag. B* **82**, 1089 (2002).